

Application of ZnO–Fe₃O₄ Nanocomposite on the Removal of Azo Dye from Aqueous Solutions: Kinetics and Equilibrium Studies

Mehrdad Farrokhi · Seyydeh-Cobra Hosseini · Jae-Kyu Yang · Mehdi Shirzad-Siboni

Received: 18 May 2014 / Accepted: 7 August 2014 / Published online: 19 August 2014
© Springer International Publishing Switzerland 2014

Abstract In this study, zinc oxide was immobilized on magnetite nanoparticles by chemical method and it was used as an adsorbent to remove reactive black 5 (RB5) dye from aqueous solution. The removal efficiency of RB5 was studied as the function of adsorbent dosage, pH, initial RB5 concentration, H₂O₂, and ionic strength (sodium carbonate, sodium bicarbonate, sodium sulfate, and sodium chloride). Removal efficiency of RB5 by ZnO–Fe₃O₄ was greater than that by ZnO and Fe₃O₄ in similar conditions. Maximum adsorption of ZnO–Fe₃O₄ was obtained at neutral pH, and adsorption capacity was estimated to be 22.1 mg/g. Adsorption kinetic study revealed that the pseudo-second-order model better described the removal rate than the pseudo-first-order

model. Adsorption isotherm was analyzed by both Langmuir and Freundlich equations, and results showed that it was better described by the Langmuir equation. The removal efficiency of RB5 was increased with increasing initial H₂O₂ concentrations from 2 to 5 mM but was decreased above 5 mM. The adsorption capacities of RB5 was increased in the presence of NaCl but was greatly decreased in the presence of bicarbonate, carbonate, and sulfate ion. Adsorption activity of RB5 by ZnO–Fe₃O₄ composite was maintained even after five successive cycles, suggesting a promising adsorbent for wastewater-contaminated organic dyes.

Keywords Nanocomposite · ZnO–Fe₃O₄ · Kinetic models · Isotherm models · Adsorption · Reactive black 5

M. Farrokhi
Department of Environmental Health Engineering, Faculty of Health, Alborz University of Medical Sciences,
Karaj, Iran

S.-C. Hosseini
Department of Environmental Health Engineering,
School of Health, Guilan University of Medical Sciences,
Rasht, Iran

J.-K. Yang
Division of General Education, Kwangwoon University,
Seoul, Republic of Korea

M. Shirzad-Siboni (✉)
Department of Environmental Health Engineering,
School of Public Health, Iran University of Medical Sciences,
Tehran, Iran
e-mail: mshirzadsiboni@yahoo.com

1 Introduction

Organic dyes are widely used in several industries such as textile, paper, cosmetic, leather, plastic, food, printing, and pharmaceutical (Asgher 2012; Fagundes-Klen et al. 2012; Ip et al. 2010). Most common types of dyes are azo and reactive dyes (Shirzad-Siboni et al. 2014b; Daneshvar et al. 2007a, b). When the organic dyes are discharged into terrestrial and aquatic ecosystems, they can cause serious environmental problem and toxicity to organisms (Elizalde-Gonzalez and Hernandez-Montoya 2009; Elwakeel 2009). Therefore, wastewater contaminated with organic dyes should be treated with suitable physicochemical and/or biological treatment processes (Gaikwad and Kinldy 2009; Gulnaz et al. 2006; Gupta

et al. 2003). Biodegradation of textile dyes is difficult or impossible due to the stability and complexity of the aromatic structure (Camp and Sturrock 1990; Sen et al. 2011; Yagub et al. 2012). As a plausible physicochemical process (Chatterjee et al. 2007), reverse osmosis (Nataraj et al. 2009), membrane filtration (Nataraj et al. 2009; Wu et al. 1998), chemical precipitation (Zhu et al. 2007), electro-deposition (Regan and Schwartz 1995), electro-coagulation (Sengila and Ozacarb 2009), advanced oxidation (Khataee et al. 2010; Khataee and Kasiri 2010; Shirzad-Siboni et al. 2011a), and ion exchange (Raghu and Ahmed Basha 2007) have been applied. Some of these processes have several disadvantages, such as formation of hazardous byproducts, high initial installation cost, generation of chemical wastes, and high-energy requirement (Raghu and Ahmed Basha 2007; Shirzad-Siboni et al. 2011a; Zhu et al. 2007). Among several physicochemical processes, adsorption technique has been widely used because it is simple, efficient, and requires low operating cost in the removal of dyes and organic matters from wastewater (Uzun 2006). Generally, carbon-based materials have been widely used as efficient adsorbents (Al-Degs et al. 2000). However, it has a limitation in large-scale application due to the relatively high preparation cost, especially activated carbon (Al-Degs et al. 2000). To compensate this limitation, low-cost adsorbents including sawdust (Ferrero 2007), agricultural residues (Nigam et al. 2000), red mud and fly ash (Wang et al. 2005), dolomite (Walker et al. 2003), oyster shell (Qiu-yue et al. 2010), activated sludge (Gulnaz et al. 2006), furnace slag (Xue et al. 2009), chitosan (Barron-Zambrano et al. 2010), activated red mud (Shirzad-Siboni et al. 2014a), and scallop shell (Shirzad-Siboni et al. 2014a, b, c) have been applied to treat wastewater. Recently, highly porous nanosized materials, having ample active surface sites, have been used in the treatment of wastewater (Sun et al. 2011; Wang et al. 2012). Among various nanosized materials, ZnO and Fe₃O₄ have much attention because ZnO nanoparticles exhibit an efficient photocatalytic removal efficiency through adsorption and decomposition of organic contaminants (Behnajady et al. 2006). In addition, super paramagnetic Fe₃O₄ nanoparticles possess a promising adsorption capacity for contaminants along with optimal magnetic properties, showing rapid separation of the adsorbent from solution via a magnetic field (Chen et al. 2011; Geng et al. 2012).

Fe₃O₄-graphene oxide composite has been used in the removal of organic dyes from waste water (Ai et al. 2011; Geng et al. 2012; Sun et al. 2011; Wu et al. 2013; Xie et al. 2012). Wang et al. (2010) used magnetic Fe₃O₄ nanoparticles for the removal of acid dye. Rongcheng and Jiuhui (2004) reported removal of azo dye from water by magnetite adsorption and Fenton oxidation. Singh et al. (2013) reported Fe₃O₄ embedded ZnO nanocomposites for the removal of toxic metal ions, organic dyes, and bacterial pathogens. Wang et al. (2010) reported removal of Rhodamine B by H₂O₂ activated by Fe₃O₄ magnetic nanoparticles. However, a limited information is available for the removal efficiency and removal kinetics of azo dye with ZnO-Fe₃O₄ composite.

Hence, in this paper the adsorption of reactive black 5 (RB5) using zinc oxide immobilized on magnetite nanoparticles was considered in aqueous solutions. The effects of adsorbent dosage, pH, initial RB5 concentrations, hydrogen peroxide, and ionic strength (sodium carbonate, sodium bicarbonate, sodium sulfate, and sodium chloride) in different time intervals on the removal efficiency were studied. Adsorption isotherm and kinetic studies were undertaken to comprehend the adsorption mechanism and maximum adsorption capacity of ZnO-Fe₃O₄ composite.

2 Materials and Methods

2.1 Chemicals

Zinc chloride (99.5 %), sodium hydroxide, hydrogen peroxide, sodium chloride, sodium sulfate, sodium hydrogen carbonate, sodium carbonate, and hydrochloric acid, which were of analytical grade, were purchased from Merck, Germany and used without any purification. Nanopowder (Fe₃O₄) was obtained from the Iranian Nanomaterial Pioneer Company in Mashhad city from Iran. It has an approximately spherical shape, is nonporous, and has greater than 99.5 % purity. The specific surface area of the Fe₃O₄ particles was known as 81.98 m²/g by company. The average size of the spherical particles was 15–20 nm. RB5 was purchased from Alvan Sabet Co., Iran. The chemical structure of RB5 has been presented in Table 1. The initial pH of solution was adjusted by the addition of 0.1 M NaOH or HCl and measured by pH meter (Metron, Switzerland). The experiments were carried out at room temperature

Table 1 The structure and characteristics of reactive black 5

Color index name	Reactive black 5
Chemical structure	
Chemical class	Anionic, diazo
Molecular formula	C ₂₆ H ₂₁ Na ₄ N ₅ O ₁₉ S ₆
Color index number	20505
λ_{\max} (nm)	597
M _w (g/mol)	991.8
Reactive group	Sulfatoethylsulfone
Natural pH	5.8

(25±2 °C). RB5 stock solution (1,000 mg/L) was prepared in distilled water and kept in the dark.

2.2 Immobilization of ZnO Nanoparticles on Fe₃O₄ Nanoparticles

Fe₃O₄ was dried at 103°C for 3 h in an oven. ZnCl₂ was used as a starting agent, and NaOH was used as a precipitant. A stock solution of 0.1 M ZnCl₂ was prepared by dissolution of ZnCl₂ into deionized water. Then an alkaline stock solution of 0.2 M NaOH was prepared in deionized water. Fe₃O₄ was added to the ZnCl₂ solution in the volume ratio of 1:1. The synthetic reaction was fundamentally performed with stirring for 7 h. The products in aqueous solution were centrifuged (4,000 rpm; Sigma-301, Germany), washed with deionized water, and then dried at 100 °C for 3 h (Shirzad-Siboni et al. 2013a). The point of zero charge (pH_{pzc}) was determined to investigate the surface charge properties of the adsorbents. The pH_{pzc} of ZnO–Fe₃O₄ composite was determined using the procedure as follows (Shirzad-Siboni et al. 2014a, b, c): a 1-L solution of 0.1 M NaNO₃ was prepared and divided into ten solutions with pH ranging from 2 to 11 adjusted by HCl and NaOH with suitable molarity. Thereafter, 0.2 g of the ZnO–TiO₂ composite was added to the solutions. The mixture was shaken at 170 rpm for 48 h. Then, the samples were centrifuged, and the pH of each solution was measured. The final pH values versus initial pH values were plotted to obtain pH_{zpc}. The pH_{pzc} can be determined at the point where the line of final pH is crossing the line of the initial pH.

2.3 Characterization Instruments

The X-ray diffraction (XRD) studies were performed with a Philips XRD instrument (Siemens D-5000, Germany) using Cu K α radiation ($\lambda=1.5406$ Å) at wide-angle range (2θ value 4–70°), an accelerating voltage of 40 kV, and an emission current of 30 mA. For characterization of the functional groups on the surface of the samples, Fourier transform infrared spectroscopy (FT-IR) spectra were recorded on a Perkin-Elmer (Germany) spectrometer under a dry air at room temperature by the KBr pellets method. The spectra were collected over the range from 400 to 4,000 cm⁻¹. The surface morphology of ZnO, Fe₃O₄, and ZnO–Fe₃O₄ composite were obtained by field emission scanning electron microscopy (FE-SEM), which was carried out by a Mira microscope (Mira3, Tescan, Czech Republic). SEM images were further supported by energy dispersive X-ray (EDX) microanalysis to provide direct evidence for the purity, existence, and distribution of specific elements in a solid sample.

2.4 Adsorption Experiments

The adsorption experiments were carried out in 1,000 mL Erlenmeyer flask containing 30 mL of RB5 solution and 2 g of ZnO–Fe₃O₄ powder, while the mixtures were stirred at 150 rpm and room temperature (25±2 °C) in different time intervals (2–60 min). Then, the samples were centrifuged (Sigma-301, Germany) at 4,000 rpm for 10 min to remove the adsorbent. The concentration of the RB5 in each sample was measured using a spectrophotometer (UV/Vis Spectrophotometer, Hach-DR 5000,

USA) at $\lambda_{\max}=597$ nm by a calibration curve, which was depicted based on Beer-Lambert law (Horwitz 2000). In order to determine the effects of various parameters, the experiments were conducted at different adsorbent amounts of 0.4 to 2 g/L, initial RB5 concentrations of 10 to 200 mg/L and initial pH of 3 to 11. Removal efficiency of RB5 dye was calculated with Eq. 1.

$$\text{Removal efficiency \%} = \frac{(C_i - C_0)}{C_i} \times 100 \quad (1)$$

where, C_i and C_0 are the initial and equilibrium concentrations of RB5 dye (mg/L), respectively.

3 Results and Discussion

3.1 Adsorbent Characterization

3.1.1 FT-IR Analysis

The functional groups on the surface of adsorbent can play a significant role in the adsorption process because adsorption reactions mostly occur on surface of the adsorbent. Thus, FT-IR analysis of ZnO, Fe₃O₄, and ZnO–Fe₃O₄ composite were performed in the range of 400–4,000 cm⁻¹ (Fig. 1). The synthesized ZnO nanorods showed significant absorption peaks at 458, 727, 913, and 3,500 cm⁻¹. The band observed between 400 and 500 cm⁻¹ corresponds to the stretching vibration of ZnO. The weak band near 1,590 cm⁻¹ is assigned to H–O–H bending vibration mode due to the adsorption of moisture when FT-IR sample disks were prepared in an open-air atmosphere. The band at 3,500 cm⁻¹ corresponds to the presence of hydroxyl groups (–OH) (Shirzad-Siboni et al. 2013a). For the case of Fe₃O₄ nanoparticles, a single sharp absorption peak at 577 cm⁻¹, attributed to Fe–O bond vibration (Sun et al. 2011; Wang et al. 2012), is observed. FT-IR spectra of ZnO–Fe₃O₄ composite were quite similar with that of ZnO, indicating hybridization of ZnO nanorods with Fe₃O₄.

3.1.2 XRD Analysis

The XRD patterns of ZnO, Fe₃O₄, and ZnO–Fe₃O₄ composite are illustrated in Fig. 2. The patterns exhibit crystalline structure of both ZnO and Fe₃O₄ even after the immobilization of ZnO on Fe₃O₄. The main peaks at 2θ values of 31.72, 34.4, 36.2, 47.49, 56.51, 62.8, 66.28,

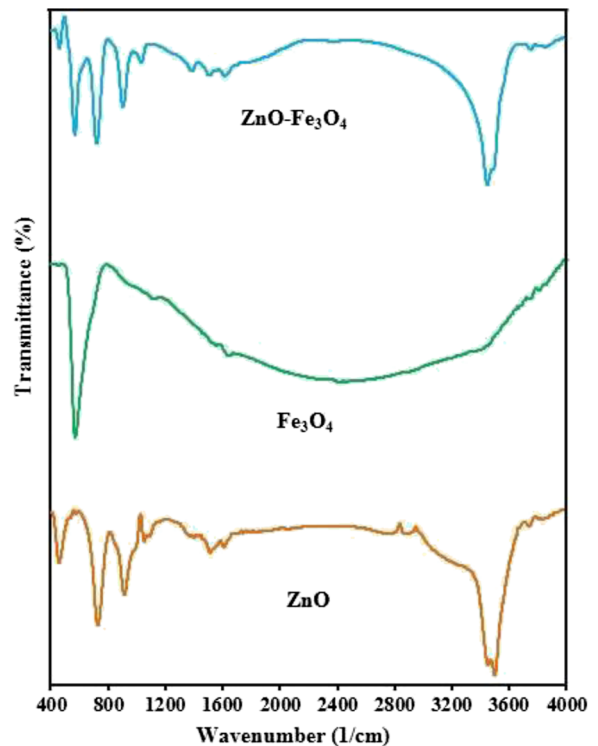


Fig. 1 FT-IR spectra of three adsorbents

67.86, and 68.86 correspond to the (100), (002), (101), (102), (110), (103), (200), (112), and (201) planes of hexagonal wurtzite ZnO (JCPDS card no. 36–1451) (Daneshvar et al. 2007b). The main peaks at 2θ values of 18.27, 21.16, 30.11, 30.21, 35.42, 35.53, 37.03, 37.18, 43.12, and 57.09 correspond to the (011), (002), (112), (200), (121), (103), (022), (202), (004), and (321) planes of the orthorhombic Fe₃O₄ (JCPDS card no. 031156) (Ai et al. 2011). As illustrated in Fig. 2, after immobilization of ZnO, the peaks related to the ZnO are still observed, which indicates growth of the ZnO crystal on the Fe₃O₄ nanoparticles.

The average crystalline size of ZnO–Fe₃O₄ composite was calculated using the following Debye–Scherrer’s equation (Patterson 1939):

$$D = \frac{0.9\lambda}{\beta \cos \theta} \quad (2)$$

where D is the average crystallite size (Å), λ is the wavelength of the X-ray radiation (Cu K α =1.54178 Å), β is the full width at half maximum intensity of the peak, and θ is the diffraction angle (18.195). According to Eq. 2, the mean crystallite size of the ZnO–Fe₃O₄ composite was estimated to be about 40 nm

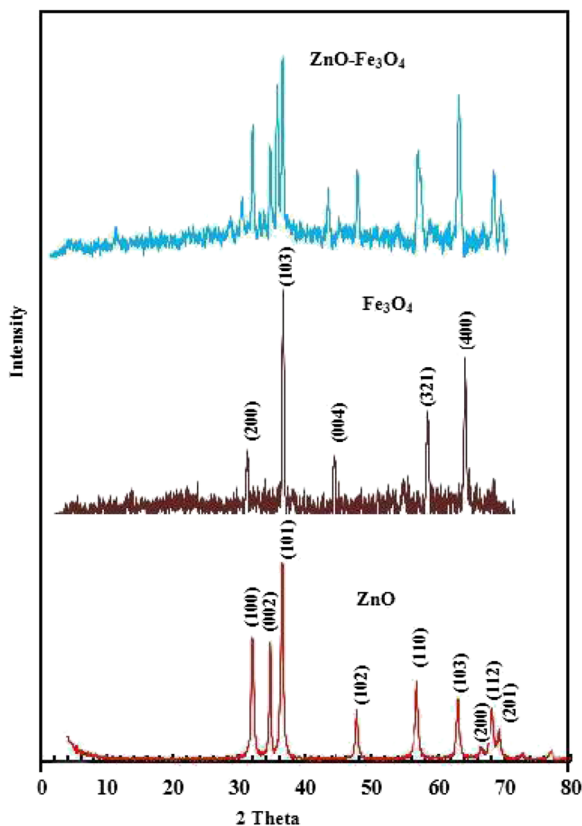


Fig. 2 Typical XRD patterns of three adsorbents

3.1.3 SEM and EDX Analyses

SEM images of ZnO nanoparticles, Fe₃O₄ nanoparticles, and ZnO–Fe₃O₄ composite are shown in Fig. 3a–c, respectively. ZnO was shaped as rods as shown in Fig. 3a, c. As shown in Fig. 3b, c, ZnO–Fe₃O₄ composite was composed of spherical Fe₃O₄ nanoparticles and ZnO nanorods. EDX microanalysis was used to characterize the elemental composition of the ZnO–Fe₃O₄ composite. EDX pattern of the ZnO–Fe₃O₄ composite is depicted in Fig. 4. According to the results of EDX analysis, the major elements were Zn, O, and Fe, indicating good hybridization between ZnO and Fe₃O₄.

3.2 Removal of Reactive Black 5

3.2.1 The Effect of Adsorbent Dosage and Contact Time

The influence of adsorbent dosage on the removal efficiency for RB5 was investigated at various amounts of adsorbents in the range of 0.4–2 g/L at pH 7 with variation of reaction time (Fig. 5). RB5 removal efficiency

was increased by increasing the adsorbent dosage from 0.4 to 2 g/L over the entire reaction time (2–120 min). This trend can be explained by the increased active sites for the removal of contaminants along with the increase of the adsorbent dosage (Shirzad-Siboni et al. 2013b, 2014a, b, c). As shown in Fig. 5, the removal rate of RB5 for all dosages was rapid in the first stages of contact time, and then it was gradually slowed until reactions reach a near equilibrium after 60 min. The rapid adsorption at initial reaction time may be attributed to the abundance of free active sites on the surface of ZnO–Fe₃O₄ and easy availability of them for RB5 molecules. As the active sites are occupied by RB5, adsorption rates are decreased due to having little available active sites on the adsorbents (Ip et al. 2010).

3.2.2 The Effect of Solution pH and Comparison of RB5 Removal by Three Adsorbents

The effect of pH on the RB5 adsorption onto ZnO–Fe₃O₄ was investigated between pH 3 and 11, and the results are depicted in Fig. 6a. According to Fig. 6a, the solution pH is recognized as one of the important parameters that governs the adsorption process. Generally, surface charge of the adsorbents and speciation of ionic contaminants is variable with variation of solution pH. Maximum removal efficiency of RB5 was observed at pH 7. When the initial pH was increased from 7 to 11, the RB5 removal efficiency was decreased from 87.55 to 20.42 %. Also as the initial pH was decreased from 7 to 3, the RB5 removal efficiency was decreased from 87.55 to 78.42 %.

Removal of RB5 by three different adsorbents such as ZnO, Fe₃O₄, and ZnO–Fe₃O₄ was investigated at pH 7. Figure 6b shows that removal of RB5 was relatively low in the presence of ZnO and Fe₃O₄. However, in the presence of ZnO–Fe₃O₄ composite, 87.55 % of the RB5 was eliminated after 120 min.

In order to obtain information about the surface charge of the adsorbent, the pH of zero-point charge (pH_{ZPC}) was determined. The plot of final pH versus initial pH of the solutions is illustrated in Fig. 7. The pH_{ZPC} can be determined at the point where the line of final pH is crossing the line of initial pH. According to the data, the pH_{ZPC} of ZnO–Fe₃O₄ composite is 6. This means that at pH values below 6, the ZnO–Fe₃O₄ surface has a net positive charge, while at pH greater than 6, the surface has a net negative charge.

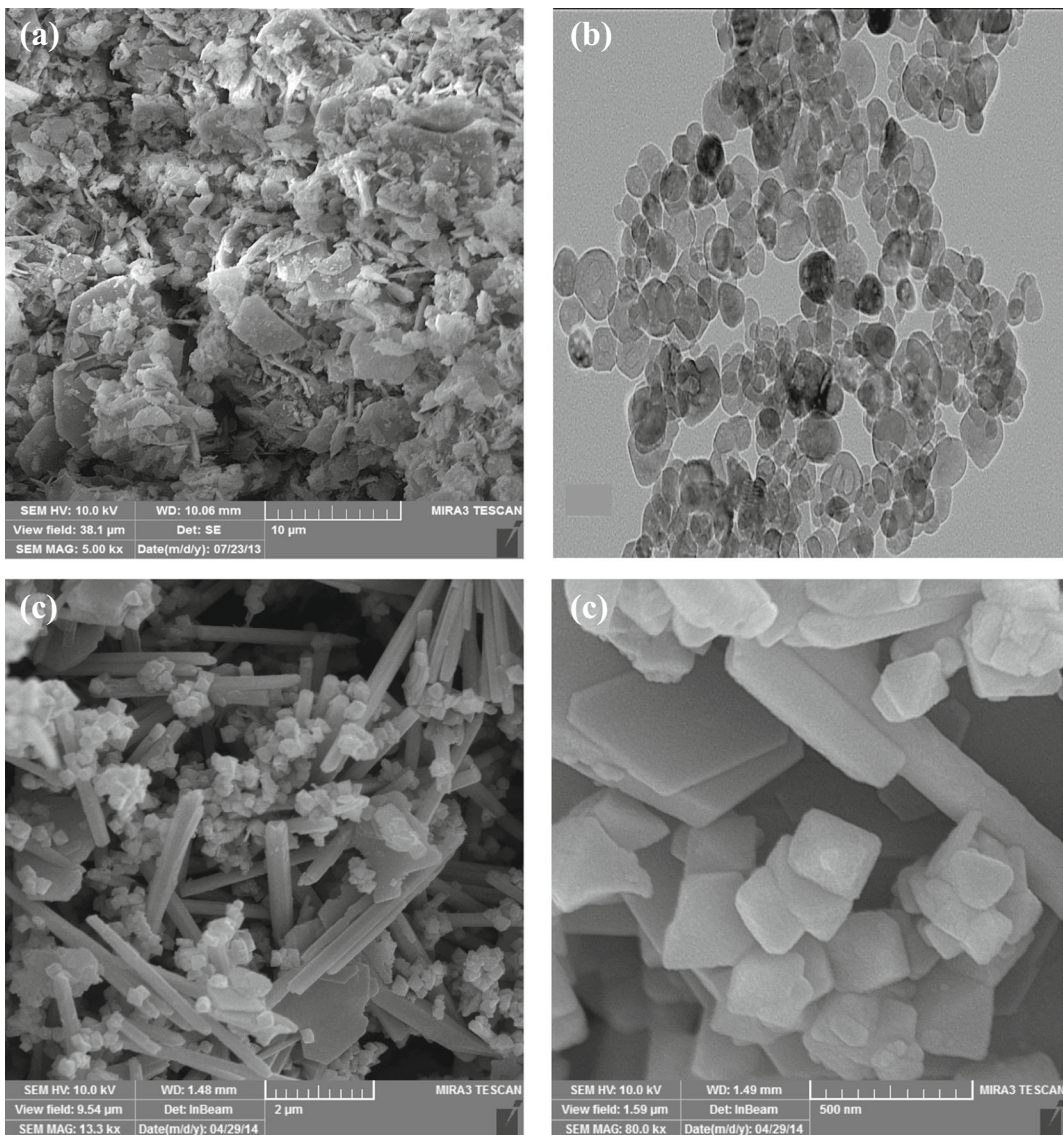


Fig. 3 SEM image of **a** ZnO, **b** Fe₃O₄, and **c** ZnO-Fe₃O₄ composite

3.2.3 The Effect of Initial RB5 Concentration

The adsorption of RB5 by ZnO-Fe₃O₄ was investigated by varying initial concentrations of RB5 ranging from 10 to 200 mg/L at pH 7 (Fig. 8). When the initial RB5 concentration was increased from 10 to 200 mg/L, the RB5 removal efficiency was decreased from 99.99 to 17.48 %. The reason for this result can be explained with the fact that the adsorbent has a limited number of active sites, which would become saturated above a certain RB5 concentration (Ip et al. 2010). Similar observations

were also reported for the removal of RB5 and herbicide (Barron-Zambrano et al. 2010; Elwakeel 2009; Eren and Acar 2006).

3.3 Kinetic and Isotherm Studies

Adsorption kinetic experiments were carried out by agitating RB5 solutions (10–200 mg/L) containing 2 g/L of ZnO-Fe₃O₄ composite for various contact times (2–120 min) at pH 7 and room temperature (25±2 °C). The pseudo-first- and pseudo-second-order models were applied in order to find an

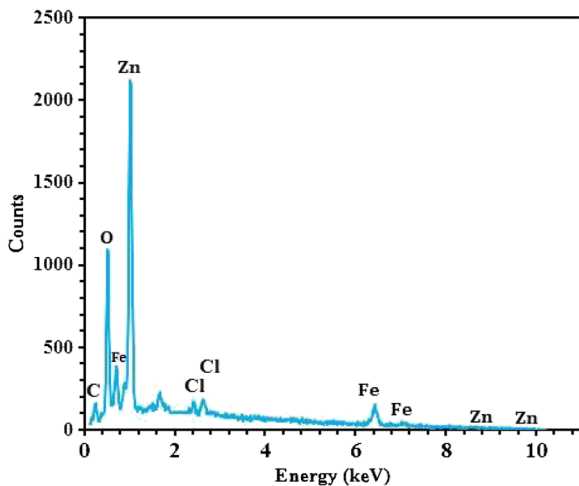


Fig. 4 EDX image of ZnO-Fe₃O₄ composite

efficient model for the description of adsorption. The relevant equations for the pseudo-first- and pseudo-second-order models were Eqs. 3 and 4, respectively (Shirzad-Siboni et al. 2011b; Samarghandi et al. 2011; Azizian 2004).

$$\log(q_e - q_t) = \log q_e - \left(\frac{k_1}{2.303}\right)t \quad (3)$$

$$\frac{t}{q_t} = \left(\frac{1}{k_2 q_e^2}\right) + \left(\frac{1}{q_e}\right)t \quad (4)$$

where q_e and q_t are the amounts of the RB5 adsorbed by ZnO-Fe₃O₄ (mg/g) at equilibrium and after reaction

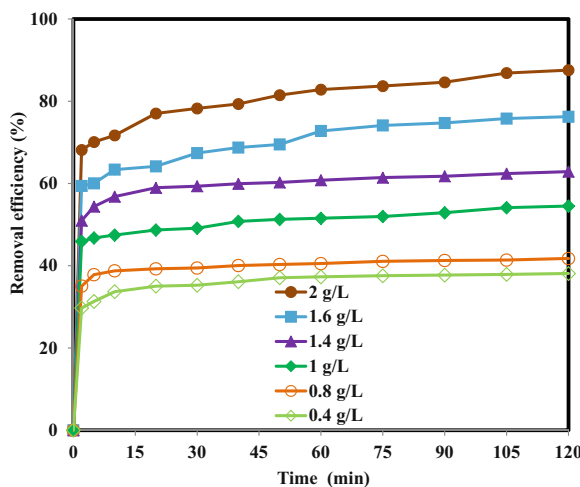


Fig. 5 Effect of adsorbent dose on the removal of RB5 dye by ZnO-Fe₃O₄ (initial dye concentration=30 mg/L, pH=7)

time t , respectively, and k_1 (1/min) and k_2 (g mg⁻¹ min⁻¹) are the pseudo-first- and pseudo-second-order rate constants, respectively. The estimated kinetic parameters for RB5 are summarized in Table 2. The kinetic data for RB5 adsorption showed the best fitting ($R^2=0.9986$) with the pseudo-second-order model. Moreover, when the initial RB5 concentration increased from 10 to 200 mg/L, the value of R^2 for the pseudo-second-order model was decreased and the value of q_e increased, indicating that adsorption data were in agreement with this model. The results are consistent with previous literatures in which the adsorption kinetic data of RB5 by different adsorbents were fitted with the pseudo-second-order model. Also,

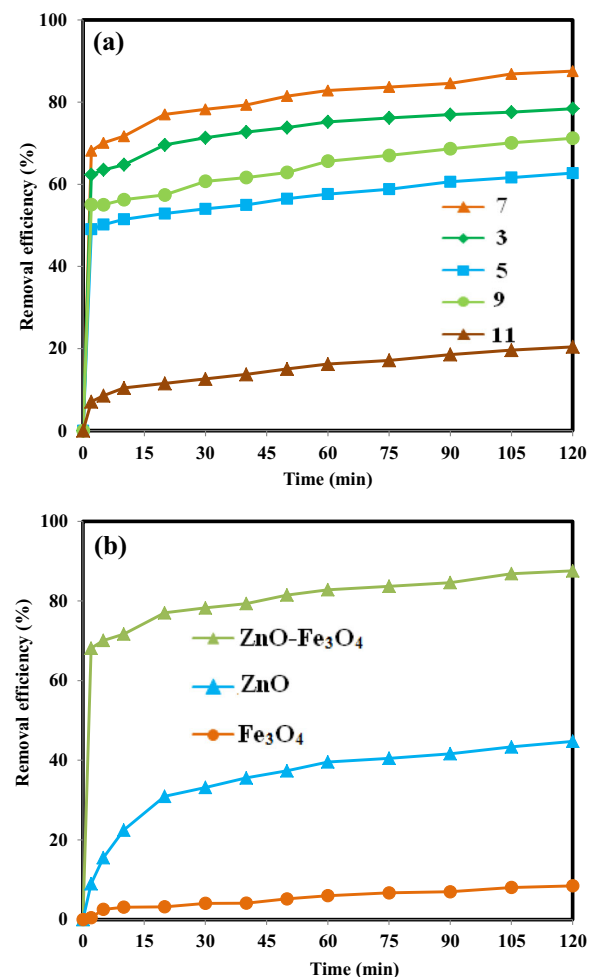


Fig. 6 a Effect of pH on the removal of RB5 dye by ZnO-Fe₃O₄ at different time intervals (initial dye concentration=30 mg/L, adsorbent dose=2 g/L) and b comparison of RB5 removal by three adsorbents (pH=7, initial dye concentration=30 mg/L, adsorbent dose=2 g/L)

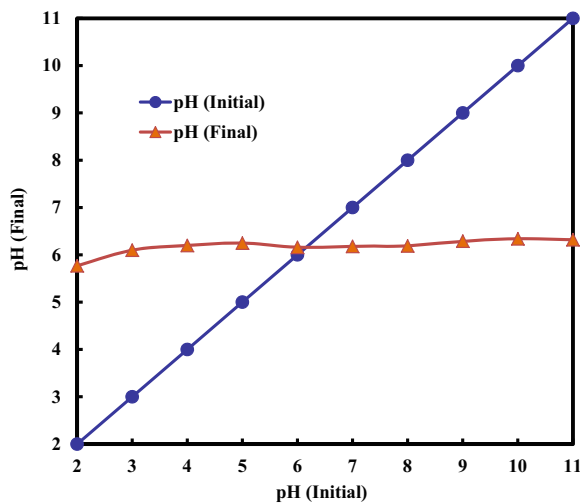


Fig. 7 Determination of the pH of point of zero charge (PZC)

the kinetic data were fitted with the linear regression statistics method. The estimated *P* values for RB5 are summarized in Table 2. From these results, kinetic data for RB5 adsorption was fitted well with the pseudo-second-order model ($P < 0.05$) compared with pseudo-first-order model.

To investigate the adsorption equilibrium isotherm, experiments were performed with 30 mg/L RB5 as an initial concentration using various adsorbent dosages (0.01–0.2 g/L) at pH 7 for 24 h. All experiments were repeated three times, and the average values were reported. Langmuir and Freundlich equations were applied to fit experimental adsorption data, and the related equations are described by Eqs. 5 and 6, respectively

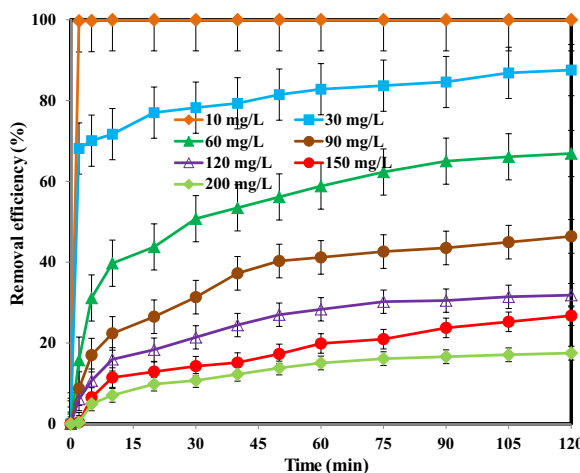


Fig. 8 Effect of initial dye concentration on the removal of RB5 dye by ZnO–Fe₃O₄ (pH=7, adsorbent dose=2 g/L)

(Azizian 2004; Samarghandi et al. 2011; Shirzad-Siboni et al. 2011b).

$$q_e = \frac{K_L q_m C_e}{1 + K_L C_e} \tag{5}$$

$$\log q_e = \log K_F + \frac{1}{n} \log C_e \tag{6}$$

where q_m (mg/g) is the maximum monolayer adsorption capacity, C_e is the sorbate concentration in solution at equilibrium (mg/L), K_L (L/mg) and K_F ($\text{mg}^{1-1/n} \text{L}^{1/n} \text{g}^{-1}$) are the Langmuir and Freundlich constants, respectively, and n is the intensity of adsorption. The estimated Freundlich and Langmuir constants as well as related correlation coefficients are summarized in Table 3. The high correlation coefficient ($R^2=0.992$) confirmed the plausible applicability of the Langmuir model for the RB5 adsorption process onto ZnO–Fe₃O₄ composite. It means that the adsorption of RB5 onto ZnO–Fe₃O₄ composite occurred as homogeneous and monolayer adsorption.

The removal capacity of RB5 by ZnO–Fe₃O₄ composite was compared with that by other adsorbents in Table 3. ZnO–Fe₃O₄ composite has greater adsorption capacity than other adsorbents. Maximum adsorption capacity was obtained 22.1 mg/g at pH 7. Based on the obtained results, the ZnO–Fe₃O₄ composite can be regarded as an efficient and low-cost adsorbent.

3.4 Effect of Ionic Strength

To assess the effect of the presence of different ionic strengths on the removal efficiency of RB5, constant amounts of sodium chloride, sodium sulfate, sodium bicarbonate, and sodium carbonate were added to the batch system before beginning the adsorption. The concentration of each ionic strength was adjusted to 30 mg/L, while the initial RB5 concentration, ZnO–Fe₃O₄ dosage, initial pH were constant at 30 mg/L, 2 g/L, and 7, respectively. Figure 9 shows that order of removal efficiency of RB5 is sodium chloride > control > sodium sulfate > sodium bicarbonate > sodium carbonate. The removal efficiency of RB5 was greatly decreased in the presence of background electrolytes having sulfate, bicarbonate, and carbonate anions compared with control test without background electrolytes. On the other hand, removal percentage of RB5 in the presence of sodium chloride was greater than control test. This removal trend can be explained by the fact that CO_3^{2-} , HCO_3^- ,

Table 2 The calculated kinetic parameters for the pseudo-first- and pseudo-second-order models for the removal of RB5 dye by ZnO–Fe₃O₄

(RB5) ₀ (mg/L)	<i>q_e</i> (exp) (mg/g)	Pseudo-first-order model				Pseudo-second-order model			
		<i>k</i> ₁ (1/min)	<i>q_e</i> (cal) (mg/g)	<i>R</i> ²	<i>P</i> value	<i>k</i> ₂ (g mg ⁻¹ min ⁻¹)	<i>q_e</i> (cal) (mg/g)	<i>R</i> ²	<i>P</i> value
10	4.99	0.0955	5.00	0.8855	0.0001	6.66	5.00	0.9999	0.033
30	13.1	0.0384	13.1	0.7905	0.024	3.49×10 ⁻²	13.1	0.9986	0.03
60	20.1	0.0444	20.1	0.8943	0.941	0.99×10 ⁻²	20.9	0.9923	0.0001
90	20.9	0.0411	20.1	0.8426	0.933	0.42×10 ⁻²	22.1	0.9890	0.0001
120	19.1	0.0384	19.2	0.9714	0.680	0.41×10 ⁻²	20.9	0.9875	0.0001
150	20.1	0.0411	20.1	0.6682	0.484	0.26×10 ⁻²	20.9	0.9379	0.001
200	17.5	0.0543	17.5	0.7214	0.443	0.38×10 ⁻²	18.8	0.9761	0.0001

and SO₄²⁻ may interfere or compete the electrostatic attraction between SO₃⁻ ions in RB5 species and surface of ZnO–Fe₃O₄ composite (Elwakeel 2009; Eren and Acar 2006).

3.5 Effect of the Hydrogen Peroxide (H₂O₂–ZnO–Fe₃O₄ or Fenton Process)

Effect of the H₂O₂ concentration on the removal of RB5 by ZnO–Fe₃O₄ composite was studied at different H₂O₂ concentrations from 2 to 50 mM at 30 mg/L dye concentration, 2 g/L ZnO–Fe₃O₄, and pH 7. As shown in Fig. 10, the removal efficiency of RB5 was increased with increasing initial H₂O₂ concentrations from 2 to 5 mM but was decreased above 5 mM. Removal percentage of RB5 without presence of H₂O₂ increased from 68.15 % at 2 min to 87.55 % at 120 min. Removal percentage of RB5 in the presence of 2 and

5 mM H₂O₂ was increased from 74.64 to 99.99 % and from 93.75 to 99 % by increasing time from 2 to 120 min, respectively. The increased removal efficiency of RB5 after addition of H₂O₂ was attributed to the increased reaction between H₂O₂ and electron in the conduction band of ZnO–Fe₃O₄. According to Eqs. 7 and 8, H₂O₂ can effectively inhibit the electron–hole recombination. Since H₂O₂ is a better electron acceptor than dissolved oxygen, it could act as an alternative electron acceptor to oxygen. At a low concentration of H₂O₂, inhibition of the electron–hole recombination is effectively contributed to an enhanced removal RB5. But at high dosage, H₂O₂ is a powerful scavenger of electron and ·OH. Therefore, high concentration of H₂O₂ might inhibit the reaction between RB5 and positive holes or ·OH in the valence band of ZnO–Fe₃O₄ (Wang et al. 2010; Rongcheng and Jiuhui 2004).

Table 3 Comparison of isotherm data obtained in this work with other previous works

Adsorbents	Freundlich constants			Langmuir constants			Reference
	<i>K_F</i> ((mg/g) (L/mg) ^{1/<i>n</i>})	<i>n</i>	<i>R</i> ²	<i>q_m</i> (mg/g)	<i>K_L</i> (L/mg)	<i>R</i> ²	
Activated sludge	16.1	2.69	0.878	116	5.741	0.993	Gulnaz et al. (2006)
Furnace slag	3.00	1.85	0.981	74.4	0.011	0.995	Xue et al. (2009)
Chitosan	21.9	7.08	0.924	34.5	34.84	0.999	Barron-Zambrano et al. (2010)
Activated red mud	0.130	0.58	0.982	35.6	0.002	0.798	Shirzad-Siboni et al. (2014a)
Fly ash	2.05	7.12	0.987	4.38	0.349	0.997	Sun et al. (2010)
Scallop shell	9.50	2.07	0.981	90.9	0.064	0.996	Shirzad-Siboni et al. (2014a, b, c)
Surfactant-modified activated carbon	400	4.93	0.770	100	217.6	0.860	Choi et al. (2008)
ZnO–Fe ₃ O ₄	13.1	6.84	0.863	22.1	0.695	0.992	Present study

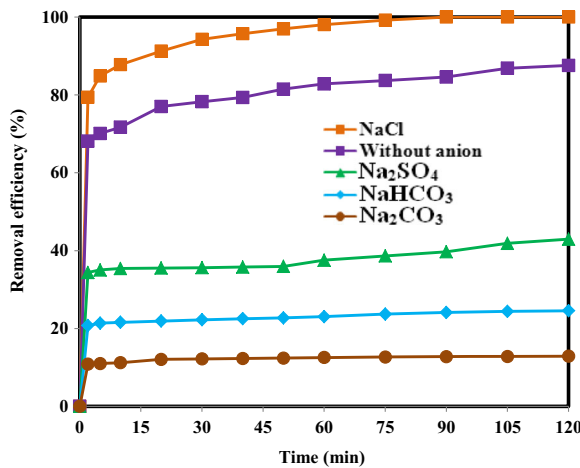
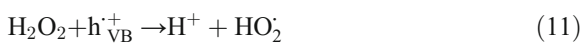
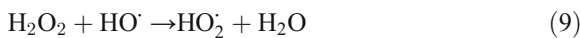


Fig. 9 Effect of ionic strength on the removal of RB5 dye by ZnO–Fe₃O₄ (pH=7, initial dye concentration=30 mg/L, adsorbent dose=2 g/L, initial ionic strength concentration=30 mg/L)



3.6 Reusability of Adsorbent

Reusability of adsorbent is an important factor for the application of developed adsorbent in the treatment of

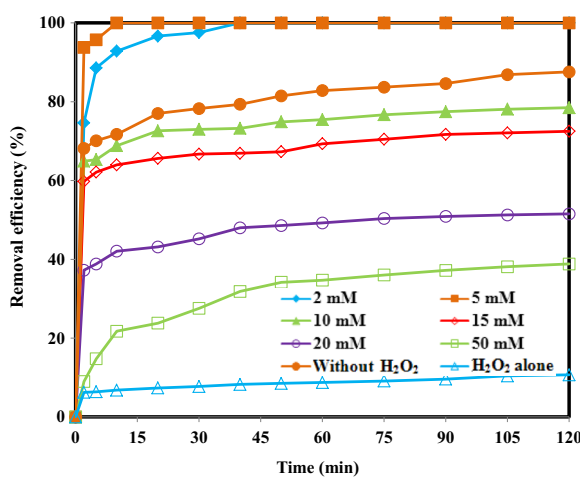


Fig. 10 Effect of H₂O₂ concentration on the removal of RB5 dye by ZnO–Fe₃O₄ (pH=7, initial dye concentration=30 mg/L, adsorbent dose=2 g/L)

wastewater. Hence, the adsorption of RB5 was performed by ZnO–Fe₃O₄ composite for five repeated runs. As can be seen in Fig. 11, adsorption capacity of RB5 by the synthesized ZnO–Fe₃O₄ composite was maintained up to five consecutive runs, suggesting a plausible adsorbent in the treatment of organic dyes.

4 Conclusions

In this research, application of ZnO immobilized on Fe₃O₄ for the adsorption of the RB5 in aqueous solutions was studied. The prepared sample was characterized by FT-IR, XRD, SEM, and EDX. Analysis of ZnO–Fe₃O₄ by FT-IR, XRD, SEM, and EDX revealed functional groups, porous surface, and essential elements, which contribute to the RB5 adsorption. The removal efficiency depended on experimental parameters like the amount of ZnO–Fe₃O₄, contact time, pH, and initial RB5 concentration. The removal efficiency was maximum at pH 7 and was increased with increase in contact time and adsorption dosage but was decreased with increase in initial dye concentration. Pseudo-second-order model better described the adsorption kinetics of RB5 onto adsorbent than the pseudo-first-order model. The high value of correlation coefficient ($R^2=0.992$) for the Langmuir isotherm suggests that adsorption occurs through homogeneous and monolayer adsorption. According to the obtained results, the

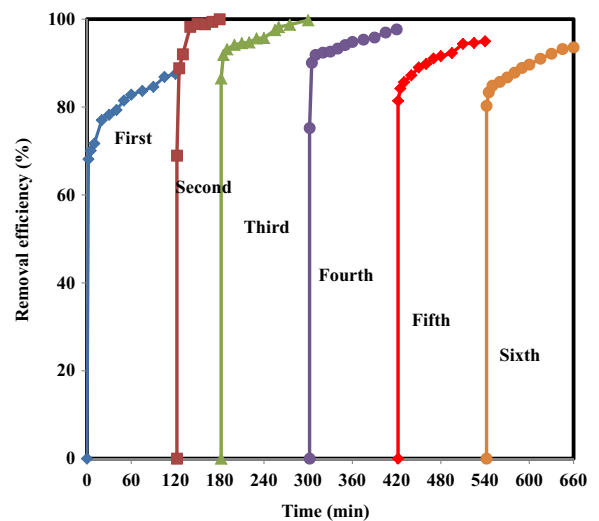


Fig. 11 Reusability test for the removal RB5 dye by ZnO–Fe₃O₄ (dosage=2 g/L, pH=7, initial dye concentration=30 mg/L)

maximum adsorption capacity of RB5 by for ZnO–Fe₃O₄ composite was 22.1 mg/g.

Acknowledgments The authors thank the Guilan, Alborz, and Iran Universities of Medical Sciences of Iran for their contributions.

References

- Ai, L., Zhang, C., & Chen, Z. (2011). Removal of methylene blue from aqueous solution by a solvothermal-synthesized graphene/magnetite composite. *Journal of Hazardous Materials*, *192*, 1515–1524.
- Al-Degs, Y., Khraisheh, M. A. M., Allen, S. J., & Ahmad, M. N. (2000). Effect of carbon surface chemistry on the removal of reactive dyes from textile effluent. *Water Research*, *34*, 927–935.
- Asgher, M. (2012). Biosorption of reactive dyes: a review. *Water, Air, & Soil Pollution*, *223*, 2417–2435.
- Azizian, S. (2004). Kinetic models of sorption: a theoretical analysis. *Journal of Colloid and Interface Science*, *276*, 47–52.
- Barron-Zambrano, J., Szygula, A., Ruiz, M., Sastre, A. M., & Guibal, E. (2010). Biosorption of reactive black 5 from aqueous solutions by chitosan: column studies. *Journal of Environmental Management*, *91*, 2669–2675.
- Behnajady, M. A., Modirshahla, N., Hamzavi, R., Behnajady, M. A., Modirshahla, N., & Hamzavi, R. (2006). Kinetic study on photocatalytic degradation of C.I. acid yellow 23 by ZnO photocatalyst. *Journal of Hazardous Materials*, *133*, 226–232.
- Camp, S. R., & Sturrock, P. E. (1990). The identification of the derivatives of C.I. reactive blue 19 in textile wastewater. *Water Research*, *24*, 1275–1278.
- Chatterjee, S., Chatterjee, S., Chatterjee, B. P., & Guha, A. K. (2007). Adsorptive removal of congo red, a carcinogenic textile dye by chitosan hydrobeads: binding mechanism, equilibrium and kinetics. *Colloids and Surfaces A: Physicochemical and Engineering Aspects*, *299*, 146–152.
- Chen, C., Gunawan, P., & Xu, R. (2011). Self-assembled Fe₃O₄-layered double hydroxide colloidal nanohybrids with excellent performance for treatment of organic dyes in water. *Journal of Materials Chemistry*, *21*, 1218–1225.
- Choi, H.-D., Shin, M.-C., Kim, D.-H., Jeon, C.-S., & Baek, K. (2008). Removal characteristics of reactive black 5 using surfactant-modified activated carbon. *Desalination*, *223*, 290–298.
- Daneshvar, N., Khataee, A. R., Rasoulifard, M. H., & Pourhassan, M. (2007a). Biodegradation of dye solution containing malachite green: optimization of effective parameters using Taguchi method. *Journal of Hazardous Materials*, *143*, 214–219.
- Daneshvar, N., Rasoulifard, M. H., Khataee, A. R., & Hosseinzadeh, F. (2007b). Removal of C.I. acid orange 7 from aqueous solution by UV irradiation in the presence of ZnO nanopowder. *Journal of Hazardous Materials*, *143*, 95–101.
- Elizalde-Gonzalez, M. P., & Hernandez-Montoya, V. (2009). Removal of acid orange 7 by guava seed carbon: a four parameter optimization study. *Journal of Hazardous Materials*, *168*, 515–522.
- Elwakeel, K. Z. (2009). Removal of reactive black 5 from aqueous solutions using magnetic chitosan resins. *Journal of Hazardous Materials*, *167*, 383–392.
- Eren, Z., & Acar, F. N. (2006). Adsorption of reactive black 5 from an aqueous solution: equilibrium and kinetic studies. *Desalination*, *194*, 1–10.
- Fagundes-Klen, M., Cervelin, P., Veit, M., Cunha Gonçalves, G., Bergamasco, R., & Silva, F. (2012). Adsorption kinetics of blue 5G dye from aqueous solution on dead floating aquatic macrophyte: effect of pH, temperature, and pretreatment. *Water, Air, & Soil Pollution*, *223*, 4369–4381.
- Ferrero, F. (2007). Dye removal by low cost adsorbents: hazelnut shells in comparison with wood sawdust. *Journal of Hazardous Materials*, *142*, 144–152.
- Gaikwad, R. W., & Kinldy, S. A. M. (2009). Studies on auramine dye adsorption on psidium guava leaves. *Korean Journal of Chemical Engineering*, *26*, 102–107.
- Geng, Z., Lin, Y., Yu, X., Shen, Q., Ma, L., Li, Z., et al. (2012). Highly efficient dye adsorption and removal: a functional hybrid of reduced graphene oxide-Fe₃O₄ nanoparticles as an easily regenerative adsorbent. *Journal of Materials Chemistry*, *22*, 3527–3535.
- Gulnaz, O., Kaya, A., & Dincer, S. (2006). The reuse of dried activated sludge for adsorption of reactive dye. *Journal of Hazardous Materials*, *134*, 190–196.
- Gupta, V. K., Ali, I., Suhas, & Mohan, D. (2003). Equilibrium uptake and sorption dynamics for the removal of a basic dye (basic red) using low-cost adsorbents. *Journal of Colloid and Interface Science*, *265*, 257–264.
- Horwitz, W. (2000). *Standard methods for the examination of water and wastewater* (20th ed.). Washington, D.C.: APHA.
- Ip, A. W. M., Barford, J. P., & McKay, G. (2010). A comparative study on the kinetics and mechanisms of removal of reactive black 5 by adsorption onto activated carbons and bone char. *Chemical Engineering Journal*, *157*, 434–442.
- Khataee, A. R., & Kasiri, M. B. (2010). Photocatalytic degradation of organic dyes in the presence of nanostructured titanium dioxide: influence of the chemical structure of dyes. *Journal of Molecular Catalysis A: Chemical*, *328*, 8–26.
- Khataee, A. R., Fathinia, M., Aber, S., & Zarei, M. (2010). Optimization of photocatalytic treatment of dye solution on supported TiO₂ nanoparticles by central composite design: intermediates identification. *Journal of Hazardous Materials*, *181*, 886–897.
- Nataraj, S. K., Hosamani, K. M., & Aminabhavi, T. M. (2009). Nanofiltration and reverse osmosis thin film composite membrane module for the removal of dye and salts from the simulated mixtures. *Desalination*, *249*, 12–17.
- Nigam, P., Armour, G., Banat, I. M., Singh, D., & Marchant, R. (2000). Physical removal of textile dyes from effluents and solid-state fermentation of dye-adsorbed agricultural residues. *Bioresource Technology*, *72*, 219–226.
- Patterson, A. (1939). The Scherrer formula for X-ray particle size determination. *Physical Review*, *56*, 978.
- Qiu-Yue, Z., Ping, Y., Yan, W., & Lei, J. (2010). Study on adsorption of Congo red in water on calcined oyster shell powder. *Technology & Development of Chemical Industry*, *48*–50.

- Raghu, S., & Ahmed Basha, C. (2007). Chemical or electrochemical techniques, followed by ion exchange, for recycle of textile dye wastewater. *Journal of Hazardous Materials*, *149*, 324–330.
- Regan, B. O., & Schwartz, D. T. (1995). Efficient photo-hole injection from adsorbed cyanine dyes into electrodeposited copper(I) thiocyanate thin films. *Chemistry of Materials*, *7*, 1349–1354.
- Rongcheng, W., & Jiuhui, Q. (2004). Removal of azo dye from water by magnetite adsorption-fenton oxidation. *Water Environment Research*, *76*, 2637–2642.
- Samarghandi, M. R., Azizian, S., Shirzad-Siboni, M., Jafari, S. J., & Rahimi, S. (2011). Removal of divalent nickel from aqueous solutions by adsorption onto modified holly sawdust: equilibrium and kinetics. *Journal of Environmental Health Science and Engineering*, *8*, 181–188.
- Sen, T., Afroze, S., & Ang, H. M. (2011). Equilibrium, kinetics and mechanism of removal of methylene blue from aqueous solution by adsorption onto pine cone biomass of pinus radiata. *Water, Air, & Soil Pollution*, *218*, 499–515.
- Sengila, I. A., & Ozacarb, M. (2009). The decolorization of C.I. reactive black 5 in aqueous solution by electrocoagulation using sacrificial iron electrodes. *Journal of Hazardous Materials*, *161*, 1369–1376.
- Shirzad-Siboni, M., Samarghandi, M., Yang, J.-K., & Lee, S.-M. (2011a). Photocatalytic removal of reactive black-5 dye from aqueous solution by UV irradiation in aqueous TiO₂: equilibrium and kinetics study. *Journal of Advanced Oxidation Technologies*, *14*, 302–307.
- Shirzad-Siboni, M., Samarghandi, M. R., Azizian, S., Kim, W. G., & Lee, S. M. (2011b). The removal of hexavalent chromium from aqueous solutions using modified holly sawdust: equilibrium and kinetics studies. *Environmental Engineering Research*, *16*, 1–6.
- Shirzad-Siboni, M., Farrokhi, M., Darvishi Cheshmeh Soltani, R., Khataee, A., & Tajassosi, S. (2013a). Photocatalytic reduction of hexavalent chromium over ZnO nanorods immobilized on kaolin. *Industrial & Engineering Chemistry Research*.
- Shirzad-Siboni, M., Jafari, S.-J., Farrokhi, M., & Yang, J. K. (2013b). Removal of phenol from aqueous solutions by activated red mud: equilibrium and kinetics studies. *Environmental Engineering Research*, *18*, 247–252.
- Shirzad-Siboni, M., Jafari, S. J., Giahi, O., Kim, I., Lee, S.-M., & Yang, J.-K. (2014a). Removal of acid blue 113 and reactive black 5 dye from aqueous solutions by activated red mud. *Journal of Industrial and Engineering Chemistry*, *20*, 1432–1437.
- Shirzad-Siboni, M., Khataee, A., & Joo, S. W. (2014b). Kinetics and equilibrium studies of removal of an azo dye from aqueous solution by adsorption onto scallop. *Journal of Industrial and Engineering Chemistry*, *20*, 610–615.
- Shirzad-Siboni, M., Khataee, A., Vafaei, F. & Joo, S. (2014b). Comparative removal of two textile dyes from aqueous solution by adsorption onto marine-source waste shell: kinetic and isotherm studies. *Korean Journal of Chemical Engineering*, 1–9.
- Singh, S., Barick, K., & Bahadur, D. (2013). Fe₃O₄ embedded ZnO nanocomposites for the removal of toxic metal ions, organic dyes and bacterial pathogens. *Journal of Materials Chemistry A*, *1*, 3325–3333.
- Sun, D., Zhang, X., Wu, Y., & Liu, X. (2010). Adsorption of anionic dyes from aqueous solution on fly ash. *Journal of Hazardous Materials*, *181*, 335–342.
- Sun, H., Cao, L., & Lu, L. (2011). Magnetite/reduced graphene oxide nanocomposites: one step solvothermal synthesis and use as a novel platform for removal of dye pollutants. *Nano Research*, *4*, 550–562.
- Uzun, İ. (2006). Kinetics of the adsorption of reactive dyes by chitosan. *Dyes and Pigments*, *70*, 76–83.
- Walker, G. M., Hansen, L., Hanna, J. A., & Allen, S. J. (2003). Kinetics of a reactive dye adsorption onto dolomitic sorbents. *Water Research*, *37*, 2081–2089.
- Wang, S., Boyjoo, Y., Choueib, A., & Zhu, Z. H. (2005). Removal of dyes from aqueous solution using fly ash and red mud. *Water Research*, *39*, 129–138.
- Wang, N., Zhu, L., Wang, M., Wang, D., & Tang, H. (2010). Sono-enhanced degradation of dye pollutants with the use of H₂O₂ activated by Fe₃O₄ magnetic nanoparticles as peroxidase mimetic. *Ultrasonics Sonochemistry*, *17*, 78–83.
- Wang, L., Li, J., Jiang, Q., & Zhao, L. (2012). Water-soluble Fe₃O₄ nanoparticles with high solubility for removal of heavy-metal ions from waste water. *Dalton Transactions*, *41*, 4544–4551.
- Wu, Eiteman, M., & Law. (1998). Evaluation of membrane filtration and ozonation processes for treatment of reactive-dye wastewater. *Journal of Environmental Engineering*, *124*, 272–277.
- Wu, Q., Feng, C., Wang, C., & Wang, Z. (2013). A facile one-pot solvothermal method to produce superparamagnetic graphene-Fe₃O₄ nanocomposite and its application in the removal of dye from aqueous solution. *Colloids and Surfaces B: Biointerfaces*, *101*, 210–214.
- Xie, G., Xi, P., Liu, H., Chen, F., Huang, L., Shi, Y., et al. (2012). A facile chemical method to produce superparamagnetic graphene oxide-Fe₃O₄ hybrid composite and its application in the removal of dyes from aqueous solution. *Journal of Materials Chemistry*, *22*, 1033–1039.
- Xue, Y., Hou, H., & Zhu, S. (2009). Adsorption removal of reactive dyes from aqueous solution by modified basic oxygen furnace slag: isotherm and kinetic study. *Chemical Engineering Journal*, *147*, 272–279.
- Yagub, M., Sen, T., & Ang, H. M. (2012). Equilibrium, kinetics, and thermodynamics of methylene blue adsorption by pine tree leaves. *Water, Air, & Soil Pollution*, *223*, 5267–5282.
- Zhu, M.-X., Lee, L., Wang, H.-H., & Wang, Z. (2007). Removal of an anionic dye by adsorption/precipitation processes using alkaline white mud. *Journal of Hazardous Materials*, *149*, 735–741.